NMR and ENDOR Conformational Studies of the Vanadyl Guanosine 5'-Monophosphate Complex in Hydrogen-Bonded Quartet Assemblies

ARTICLE *in* INORGANIC CHEMISTRY · MARCH 1995

Impact Factor: 4.76 · DOI: 10.1021/ic00111a021

2 AUTHORS, INCLUDING:

Marvin William Makinen
University of Chicago
95 PUBLICATIONS **2,097** CITATIONS

NMR and ENDOR Conformational Studies of the Vanadyl Guanosine 5′-Monophosphate Complex in Hydrogen-Bonded Quartet Assemblies[1]

Fa Shun Jiang and Marvin W. Makinen*

Department of Biochemistry and Molecular Biology, Cummings Life Science Center, The University of Chicago, 920 East 58th Street, Chicago, Illinois 60637

Received August 4, 1994[⊗]

The structure and conformation of guanosine 5′-monophosphate in hydrogen-bonded quartet assemblies have been investigated by use of the vanadyl ion (VO^{2+}) as a paramagnetic probe for EPR and electron nuclear double resonance (ENDOR) spectroscopy. EPR spectrometric titrations showed that the stoichiometry of VO^{2+}:nucleotide binding was 1:2. Proton ENDOR absorptions of the vanadyl−nucleotide complex indicated the presence of only axially coordinated H_2O in the inner coordination sphere. This result and the observation of a ^{31}P superhyperfine coupling pattern of 1:2:1 relative intensity in EPR spectra established that chelation of VO^{2+} occurs through phosphate groups in a bidentate fashion with oxygen atoms positioned in the equatorial plane to form a [VO-$(GMP)_2(H_2O)$] complex. Specific assignments of proton ENDOR absorptions were made for the purine H(8) and a ribose OH on the basis of deuterium substitution. Conditions under which [$VO(GMP)_2(H_2O)$] was incorporated predominantly into quartets or stacked quartets at 1 °C were established by NMR. Proton ENDOR spectra of frozen solutions showed identical splittings for [$VO(GMP)_2(H_2O)$] as a monomer complex or when incorporated predominantly into quartets or stacked quartets. From the principal hyperfine coupling components, dipolar electron−proton distances were calculated and applied as constraints in computer-based torsion angle search calculations. The results showed that the guanine base acquires an *anti* conformation while the ribose moiety could be accommodated only by a *C3′*-endo conformation. The results are discussed with reference to recent X-ray crystallographic and NMR studies of G-quartets formed by synthetic oligonucleotide strands of DNA and RNA.

Introduction

Guanosine and its nucleotide derivatives are unusual among the five nucleic acid components of RNA and DNA because they are capable of forming self-structured assemblies in solution through hydrogen bonding to give G−G base pairs and G-quartets.[2,3] The G-quartet assemblies are formed through a square-planar array of hydrogen-bonded guanine bases, illustrated in Figure 1. Equilibria controlling the formation of G-quartets and of stacked quartets to form octets and higher order assemblies are sensitive to pH and to the presence of sodium and potassium ions.[4−7] Fiber diffraction studies have shown that under acidic pH conditions GMP forms a helical arrangement of a continuously hydrogen-bonded ramp of guanine bases.[2,8] In the neutral and alkaline pH region, application of crystallographic,[8] spectroscopic[9,10] and calorimetric[11] methods demonstrates that G-quartets and higher order aggregates of stacked quartets are formed. The importance of G-quartets formed from mononucleosides and mononucleotides of guanine is related to the notion that the guanine-rich regions of terminal regions of DNA strands in telomeres are thought to form similar, non-Watson−Crick hydrogen-bonded quartet arrays of the guanine bases that appear to be important in chromosome stability and replication in the nucleus.[3,12,13] At present, biological examples of G-quartets in RNA are not known.

While the formation of G-quartets and of higher order aggregates of GMP in solution has been investigated by a variety of physical methods, there remain uncertainties concerning the fine structure of the ribose and guanine moieties in these assemblies. There has been no direct structural information to assign base conformation and ribose pucker or to relate the structural details of G-quartets formed from GMP in solution to those of G-quartets observed in oligonucleotides.[14−17] In the present study we demonstrate by application of NMR that GMP coordinated through the 5′-phosphate group to the vanadyl (VO^{2+}) ion forms G-quartets and stacked quartets in solution, as observed for GMP itself. By use of the vanadyl ion as a paramagnetic structural probe for EPR and electron nuclear double resonance (ENDOR[18]) spectroscopy, we assign the structure of the GMP moiety in the complex. The ENDOR spectra of the complex in solution as a monomeric unit, in

* Corresponding author.
⊗ Abstract published in *Advance ACS Abstracts,* March 1, 1995.
(1) This work was supported by a grant from the NIH (GM21900).
(2) Gellert, M.; Lipsett, M. N.; Davies, D. R. *Proc. Natl. Acad. Sci. U.S.A.* **1962**, *48*, 2013−2018.
(3) Sen, D.; Gilbert, W. *Methods Enzymol.* **1992**, *211*, 191−199.
(4) Miles, H. T.; Frazier, J. *Biochem. Biophys. Res. Commun.* **1972**, *49*, 199−204.
(5) Pinnavaia, T. J.; Miles, H. T.; Becker, E. D. *J. Am. Chem. Soc.* **1975**, *97*, 7198−7200.
(6) Pinnavaia, T. J.; Marshall, C. L.; Mettler, C. L.; Fisk, C. L.; Miles, H. T.; Becker, E. D. *J. Am. Chem. Soc.* **1978**, *100*, 3625−3627.
(7) Detellier, C.; Laszlo, P. *J. Am. Chem. Soc.* **1980**, *102*, 1135−1141.
(8) Zimmerman, S. B. *J. Mol. Biol.* **1976**, *106*, 663−672.
(9) Audet, P.; Simard, C.; Savoie, R. *Biopolymers* **1991**, *31*, 243−251.
(10) Eimer, W.; Dorfmüller, Th. *J. Phys. Chem.* **1992**, *96*, 6790−6800.
(11) Klump. H. *Ber. Bunsen-Ges. Phys. Chem.* **1976**, *80*, 121−124.
(12) Williamson, J. R.; Raghuraman, M. K.; Cech, T. R. *Cell* **1989**, *59*, 871−880.
(13) Blackburn, E. H. *Nature* **1991**, *350*, 569−573.
(14) Kang, C.; Zhang, X.; Ratliff, R.; Moyzis, R.; Rich, A. *Nature* **1992**, *356*, 126−131.
(15) Cheong, C.; Moore, P. B. *Biochemistry* **1992**, *31*, 8406−8414.
(16) Smith, F. W.; Feigon, J. *Nature* **1992**, *356*, 164−168.
(17) Wang, Y.; Patel, D. J. *Biochemistry* **1992**, *31*, 8112−8119.
(18) The following abbreviations are used: CHES, 2-(*N*-cyclohexylamino)-ethanesulfonic acid; ENDOR, electron nuclear double resonance; GMP, guanosine 5′-monophosphate; hf, hyperfine; hfc, hyperfine coupling; rf, radiofrequency.

0020-1669/95/1334-1736$09.00/0

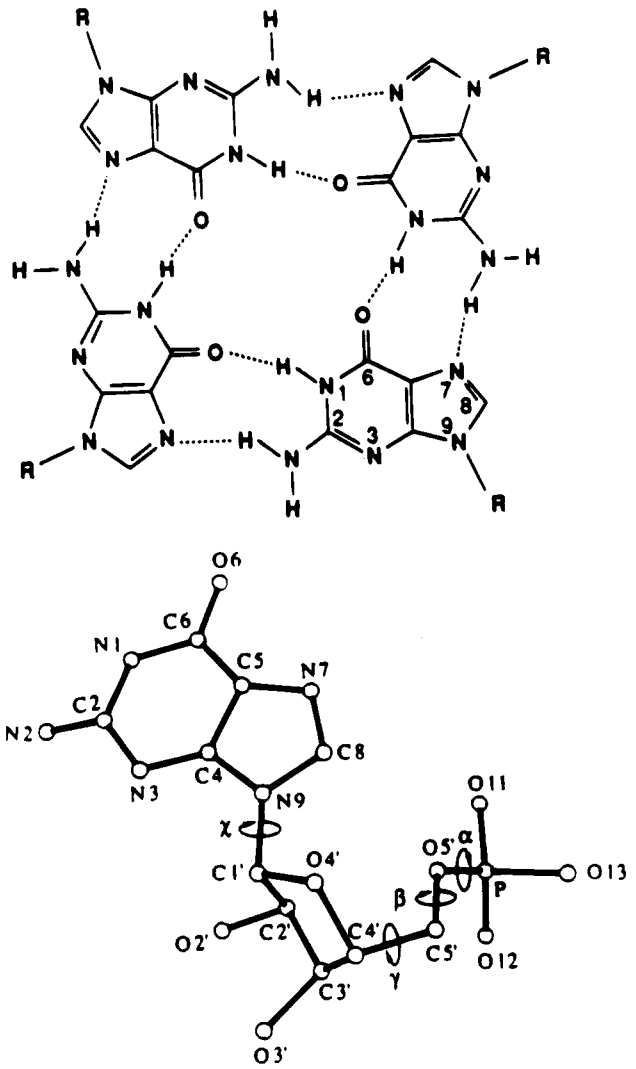

Figure 1. Top: Diagramatic illustration of the network of hydrogen bonds stabilizing guanine bases in a square-planar array of a G-quartet. Bottom: Illustration of the atomic numbering scheme for the GMP molecule and the four torsion angles which characterize its conformation.

G-quartets, and in higher order assemblies are identical, indicating that the conformation is not altered upon incorporation into these hydrogen-bonded arrays. The ENDOR data show that the base exhibits an *anti* conformation while only a *C3'-endo* conformation of the ribose moiety can be accommodated within van der Waals nonbonded limits. These studies assign the molecular conformation of GMP in solution at a level of accuracy that is exceeded only by that of X-ray diffraction studies of single crystals.

Materials and Methods

Chemicals. $VOSO_4 \cdot H_2O$, ^2H_2O (99.8 atom % ^2H), NaO^2H (>99 atom % ^2H), and ^2HCl (99 atom % ^2H) were obtained from Aldrich Chemical Co., Inc. (Milwaukee, WI 53233). CHES[18] and the disodium salt of GMP were purchased from Sigma Chemical Co. (St. Louis, MO 63178). All other reagents were of analytical grade, and deionized, distilled water was used throughout.

Preparation of [8-^{2}H]GMP. The method of Bullock and Jardetzky[19] was used to prepare [8-^{2}H]GMP by heating 1.0 g of GMP in 15 mL of ^2H_2O at 95 °C for 1.5 h. The solvent was removed by lyophilization and the procedure repeated. Analysis of the product by NMR showed greater than 95% exchange of H(8) for deuterium with no spurious resonance features. Silica gel thin-layer chromatography[20] showed only one band comigrating with a sample of untreated GMP.

(19) Bullock, F. J.; Jardetzky, O. *J. Org. Chem.* **1964**, *29*, 1988−1990.

Preparation of Samples. The pD of solutions in ^2H_2O was adjusted with ^2HCl or NaO^2H using the relationship pD = pH + 0.4, where pH is the nominal reading obtained with a glass electrode.[21] Solutions of vanadyl−nucleotide mixtures were prepared by mixing the required quantity of GMP and NaCl or KCl in 0.04 M CHES to which a slightly acidified solution of $VOSO_4$ was added under a nitrogen atmosphere. The pH (or pD) was adjusted after mixing. For EPR and ENDOR measurements, the final VO^{2+} ion concentration was generally 0.01 M and the GMP concentration varied from 0.0 to 0.1 M. All solutions containing vanadyl ions were purged with nitrogen and stored under a nitrogen atmosphere.

NMR Spectroscopy. ^1H NMR spectra were obtained with a GE GN-Omega 500 MHz Fourier transform spectrometer. ^2H_2O was used as the solvent with [$^2H_6$]acetone as the internal reference. The sample temperature was thermostated to ±0.1 °C over the −1 to +50 °C range.

EPR and ENDOR Spectroscopy. A Bruker ESP 300 E spectrometer operating at X-band microwave frequency was used for determination of EPR and ENDOR absorption spectra and was equipped with a TM_{110} cylindrical cavity, Bruker ENDOR accessory, and an Oxford Instruments ESR910 liquid helium cryostat. The radiowave source was a Wavetek signal generator (Model 3000-446) together with a frequency synthesizer (Model 160, Programmed Test Sources, Inc., Littleton, MA 01460) and rf power amplifier (Model A500 BB-1831, Electronic Navigation Industries, Inc., Rochester, NY 14623). The rf field is introduced into the cavity by a bronze wire helix with 17 turns wrapped around the quartz Dewar insert of the ESR910 cryostat. The microwave power and rf field characteristics of this ENDOR accessory system are comparable to those described earlier from this laboratory with use of a Bruker ER200D EPR spectrometer and ENDOR system.[22,23] Typical experimental conditions for EPR: sample temperature, 7 K; microwave power incident on the cavity, 0.16 mW; 12.5 kHz frequency modulation; 1.0 G amplitude modulation of the microwave field. For ENDOR measurements the following conditions were generally applied: microwave power, 6.3 mW; rf power, 60 W; modulation depth of frequency, 30 kHz or less. The static laboratory magnetic field was not modulated for ENDOR.

Molecular Modeling. The atomic coordinates of GMP were derived for non-hydrogen atoms from the X-ray-defined structures of $GMP \cdot 3H_2O$ with a *C3'-endo* ribose pucker[24] and from 8-bromoguanosine with a *C2'-endo* ribose pucker[25] while the spatial arrangements of guanosine groups in G-quartets were based on the X-ray structure of synthetic $d(G_4T_4G_4)$.[14] The positions of hydrogens were calculated on the basis of idealized valence angles and C−H bond lengths of 1.08 and 1.045 Å for sp^3- and sp^2-hybridized carbon atoms, respectively, and an O−H bond length of 1.00 Å as described previously from this laboratory.[26−28] Modeling of the VO^{2+} complex with GMP according to spectroscopic data is described below. The V=O bond length was fixed at 1.59 Å according to X-ray studies.[29] Bidentate coordination geometry of VO^{2+} with a phosphate group was based on the X-ray structure of $NaV_3P_3O_{12}$.[30]

Conformational analysis was carried out with use of the program SYBYL,[31] whereby systematic torsion angle calculations are done by

(20) Sanders, C. R., II; Tian, G.; Tsai, M. *Biochemistry* **1989**, *28*, 9028−9043.
(21) Covington, A. K.; Paabo, M.; Robinson, R. A.; Bates, R. G. *Anal. Chem.* **1968**, *40*, 700−706.
(22) Yim, M. B.; Makinen, M. W. *J. Magn. Reson.* **1986**, *70*, 89−105.
(23) Mustafi, D.; Makinen, M. W. *Inorg. Chem.* **1988**, *27*, 3360−3368.
(24) Emerson, J.; Sundaralingam, M. *Acta Crystallogr.* **1980**, *B30*, 1510−1513.
(25) Tavale, S. S.; Sobell, H. M. *J. Mol. Biol.* **1970**, *48*, 109−123.
(26) Mustafi, D.; Sachleben, J. R.; Wells, G. B.; Makinen, M. W. *J. Am. Chem. Soc.* **1990**, *112*, 2558−2566.
(27) Mustafi, D.; Telser, J.; Makinen, M. W. *J. Am. Chem. Soc.* **1992**, *114*, 6219−6226.
(28) Mustafi, D.; Boisvert, W. E.; Makinen, M. W. *J. Am. Chem. Soc.* **1993**, *115*, 3674−3682.
(29) Ballhausen, C. J.; Djurinskij, B. F.; Watson, K. J. *J. Am. Chem. Soc.* **1968**, *90*, 3305−3309.
(30) Kinomura, N.; Matsui, N.; Kumada, N.; Muto, F. *J. Solid State Chem.* **1989**, *79*, 232−237.
(31) Marshall, G. R. Personal communication. Detailed information on the use of this program package can be obtained from Tripos Associates, Inc., 1600 S. Henley Road, St. Louis, MO 63144.

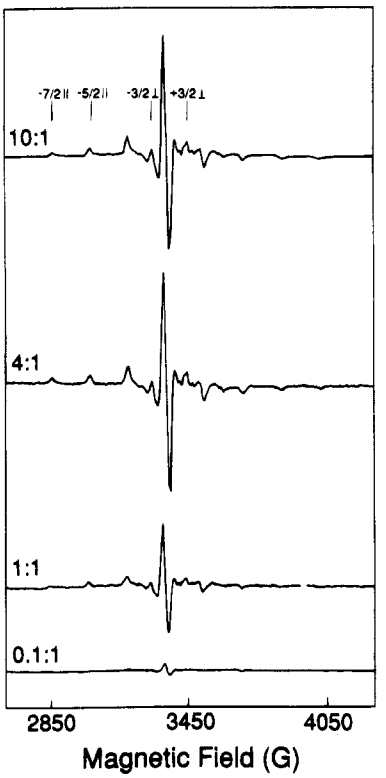

Figure 2. First-derivative EPR spectra of frozen solutions of 0.01 M VO^{2+} in 1.0 M NaCl buffered to pH 8.6 with 0.04 M CHES with different concentrations of GMP. The GMP:VO^{2+} ratio is indicated for each spectrum. In the top part of the diagram, the $-^7/_2||$, $-^5/_2||$, $-^3/_2\perp$, and $+^3/_2\perp$ resonance features are identified by vertical lines in left-to-right succession. The prominent central resonance feature in the spectrum belongs to overlapping contributions of the $-^1/_2\perp$ and the $-^1/_2||$ transitions. These EPR absorption features employed for spectroscopic analysis, as described in the text, are identified on the basis of assignments by others.[38-40]

the SEARCH option which checks for nonbonded atom contacts and scans all possible torsion angles around rotatable bonds compatible with the ENDOR-determined electron–proton distances and their respective uncertainties as added constraints. The basic elements and philosophy underlying the use of this program package have been described by Naruto *et al.*,[32] and the van der Waals radii of Iijima *et al.*[33] were applied. Molecular graphics analysis of the structures generated through the SEARCH option in SYBYL was further carried out with use of FRODO[34,35] and INSIGHT[36] running on an Evans & Sutherland PS390 graphics system with a host Digital Electronics Corp. VAX3500 computer.

Results and Discussion

EPR Characterization of VO^{2+}–GMP Complex Formation. Figure 2 illustrates frozen solution spectra of VO^{2+} added to GMP solutions. In frozen solutions, the EPR absorption spectra of VO^{2+} are characterized by an axially symmetric g matrix ($g_{||} = 1.955$ and $g_\perp = 1.977$ for solutions at pH 8.6 employed in this investigation) with eight parallel and eight perpendicular absorption features due to the ($I = ^7/_2$) ^{51}V nucleus. In the absence of chelating agents over the pH range 5–11, VO^{2+} forms an EPR-silent, polymeric $VO(OH)_2$ species.[37,38] Therefore, the observed peak-to-peak amplitudes are proportional to the concentration of VO^{2+} complexed to GMP. Identical spectra were obtained by addition of VO^{2+} to solutions of GMP buffered at pH 6 followed by adjustment of the pH to 8.6 or by addition of VO^{2+} to solutions of GMP buffered at pH 8.6. The relative peak-to-peak amplitudes in the spectrum of VO^{2+} complexed to GMP at pH 8.6 differ from that of VO^{2+} more commonly observed in acidic media,[23,39] and the spectra in Figure 2 appear more similar to that of VO^{2+} at pH $\geq$12.5.[39,40]

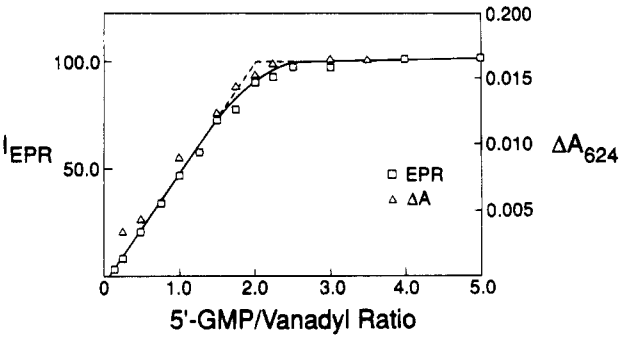

Figure 3. Spectrometric titrations of the VO^{2+} ion complexed to GMP. The EPR titration was carried out for solutions of 0.01 M VO^{2+} in 0.2 M KCl with varying GMP concentrations buffered to pH 8.6 with 0.04 M CHES. The EPR signal intensity of the central feature (*cf.* Figure 2) that exhibits the largest peak-to-peak amplitude is plotted as a function of GMP:VO^{2+} ratio. The optical titration measuring the absorbance at 624 nm was carried out with a Cary 15 recording spectrophotometer modified by On-Line Instrument Systems, Inc. (Jefferson, GA 30549), for microprocessor-controlled data collection. Solutions of 0.005 M VO^{2+}, 0.2 M KCl, and similarly varying GMP concentrations in 0.04 M 1,4-piperazinediethanesulfonic acid buffered to pH 6.7 were used. For optical titrations a lower pH was used and solutions were centrifuged to eliminate light-scattering contributions from the polymeric $VO(OH)_2$ species formed under conditions of excess VO^{2+}.

In Figure 3 the peak-to-peak amplitude for the central prominent EPR absorption feature is plotted as a function of GMP:VO^{2+} ratio. It is seen that at a 2:1 ratio the amplitude does not change further with increasing GMP concentration, indicating saturation of ligand binding with a 2:1 stoichiometry of GMP to VO^{2+}. This behavior is parallel to that of VO^{2+} binding to ADP and ATP.[27] It is also seen in Figure 3 that the stoichiometry of VO^{2+}–GMP complex formation at pH 6.7 can be monitored by optical absorption at 624 nm.

In Figure 4 is illustrated a comparison of the $+^3/_2$ perpendicular EPR absorption feature under different GMP concentration and solvent conditions. The $+^3/_2$ perpendicular EPR absorption feature of VO^{2+} at pH 12.5 is compared here to that of VO^{2+} in the presence of excess GMP at pH 8.6. In the presence of excess GMP, the $+^3/_2$ perpendicular EPR absorption exhibits a triplet feature with an approximate 21.0 G (58.9 MHz) interval spacing and relative intensity of 1:2:1. The interval spacing remains constant in ^2H_2O. A purely dipolar interaction between the vanadyl ion and the ^{31}P nucleus at a distance of ~2.5 Å would yield only an approximate 3.9 MHz contribution. We, therefore, conclude that the observed superhyperfine structure is primarily isotropic in origin and is derived from covalency. Since the isotropic hfc constant of free ^{31}P is 10178 MHz,[41] the spacing of 21.0 G (58.9 MHz) corresponds to transfer of approximately 0.5% of the unpaired spin density to

(32) Naruto, S.; Motoc, J.; Marshall, G. R.; Daniels, S. B.; Sofia, M. J.; Katzenellenbogen, J. A. *J. Am. Chem. Soc.* **1985**, *107*, 5262–5270.
(33) Iijima, H.; Dunbar, J. B., Jr.; Marshall, G. R. *Proteins: Struct., Funct., Genet.* **1987**, *2*, 330–339.
(34) Jones, T. A. In *Computational Crystallography*; Sayre, D., Ed.; Clarendon Press: Oxford, U.K., 1982; pp 303–317.
(35) Jones, T. A. *Methods Enzymol.* **1985**, *115*, 157–171.
(36) Dayringer, H. E.; Tramontano, A.; Sprang, S. R.; Fletterick, R. J. *J. Mol. Graphics* **1986**, *4*, 82–87.
(37) Francavilla, J.; Chasteen, N. D. *Inorg. Chem.* **1975**, *14*, 2860–2862.
(38) Chasteen, N. D. *Struct. Bonding (Berlin)* **1983**, *53*, 105–138.
(39) Albanese, N. F.; Chasteen, N. D. *J. Phys. Chem.* **1978**, *82*, 910–914.
(40) Ianuzzi, M. M.; Rieger, P. H. *Inorg. Chem.* **1975**, *14*, 2895–2899.
(41) Wertz, J. E.; Bolton, J. R. *Electron Spin Resonance*; McGraw-Hill: New York, 1972; p 497.

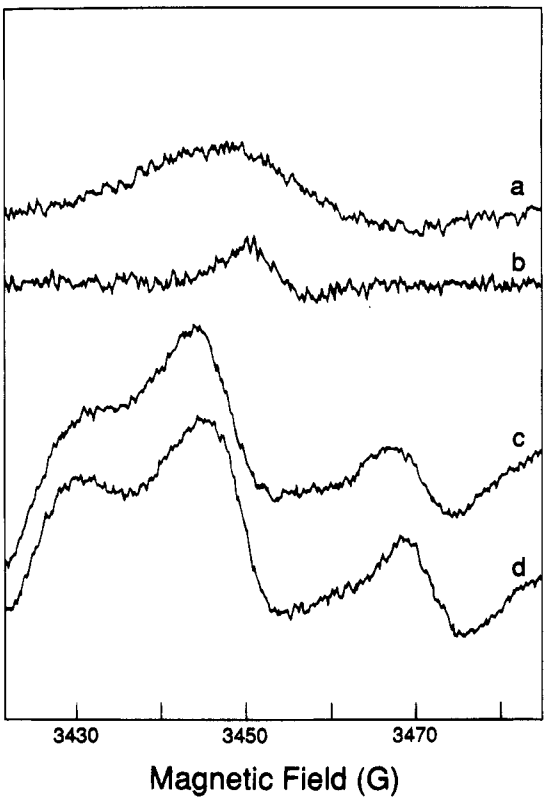

Figure 4. EPR spectra of VO^{2+} and $[VO(GMP)_2(H_2O)]$ in the region of the $+^3/_2$ perpendicular absorption feature. The following solution conditions were used: (a) 0.01 M VO^{2+} and 1.0 M NaCl at pH 12.5 in H_2O; (b) 0.01 M VO^{2+} and 1.0 M NaCl at pH 12.5 in ^2H_2O; (c) 0.01 M VO^{2+}, 0.1 M GMP, and 1.0 M NaCl at pH 8.6 in H_2O; (d) 0.01 M VO^{2+}, 0.1 M GMP, and 1.0 M NaCl at pD 8.6 in ^2H_2O. In these EPR measurements, the field modulation amplitude was 0.25 G, the scan range of the magnetic field was 100 G, and other conditions were as described under Experimental Procedures.

a pure phosphorus 3s orbital. The hfc pattern with intensity variation of 1:2:1 requires interaction of the vanadyl ion with two equivalent ($I = {}^1/_2$) ^{31}P nuclei. A similar transferred hyperfine pattern has been described by Wasson[42] for bis(*O,O'*-dialkyl dithiophosphato)oxovanadium(IV) chelates and has been assigned to two equivalent ^{31}P nuclei directly interacting with VO^{2+} in a bidentate fashion.

At GMP:VO^{2+} ratios less than 2:1, no change in the ^{31}P superhyperfine pattern was observed. We, therefore, conclude that under conditions of excess VO^{2+} a complex of only $VO(GMP)_2$ stoichiometry is formed with the excess VO^{2+} forming the EPR-silent, polymeric species. Furthermore, as seen in Figure 4, the overall line width of the $+^3/_2$ perpendicular feature is not decreased in the presence of ^2H_2O. This observation indicates that no solvent molecules (H_2O or OH^-) are bound in equatorial positions in the $VO(GMP)_2$ complex.[38,39] Together with the ENDOR evidence provided below for an axially coordinated water molecule, these results indicate that the interaction of VO^{2+} with GMP results in formation of a complex of $[VO(GMP)_2(H_2O)]$ stoichiometry.

Under conditions of identical modulation and incident microwave power for vanadyl–nucleotide mixtures at pH 8.8 and 0.6 M KCl, a detectable difference in the EPR line width was observed, dependent on GMP:VO^{2+} ratio. This difference was most readily observed for the $-^5/_2$ parallel absorption feature as a well-separated feature. For instance, for mixtures containing 0.1 M GMP and 0.01 M VO^{2+}, the line width at half-maximum amplitude was 32.1 G for the $-^5/_2$ parallel EPR absorption feature under nonsaturating levels of incident microwave power while this increased to 38.7 G for mixtures containing 0.1 M GMP and 0.04 M VO^{2+}. For VO^{2+} at pH 2 (added as $VOSO_4$), under which conditions only the $[VO(H_2O)_5]^{2+}$ complex is formed, the line width of the VO^{2+} ion remained independent of metal ion concentration over the 0.004–0.04 M range.[43] The increase in line width is best ascribed to spin–spin interactions of VO^{2+} ions. We shall demonstrate later that VO^{2+} complexed to GMP forms self-structured hydrogen-bonded G-quartets similar to that for free GMP. The increase in EPR line width is, thus, consistent with spin–spin interactions of VO^{2+} centers within the same or between stacked quartets. This observation suggests that under GMP:VO^{2+} conditions of 2.5:1, as in the case of solutions with 0.1 M GMP and 0.04 M VO^{2+}, there is on average more than one VO^{2+} ion per quartet while at higher GMP:VO^{2+} ratios there is at most only one VO^{2+} ion. This observation will be discussed later with respect to the results of modeling studies.

NMR Characterization of GMP Assemblies. It has been shown in NMR[5,7,44] and calorimetric[11] studies that aggregation of GMP proceeds according to an equilibrium involving the formation of G-quartets and stacked quartets at neutral and alkaline pH. Lowering of the temperature or the presence of potassium ions favors stacking of G-quartets into octets and higher order aggregates. On this basis, since ENDOR spectroscopy for structural analysis requires solid polycrystalline or frozen solution systems, we have employed NMR to assess the aggregation behavior of $VO(GMP)_2$ complexes near the freezing point of their aqueous solutions.

In Figure 5 we have compared the temperature dependence of NMR spectra of GMP and $[VO(GMP)_2(H_2O)]$ under conditions favoring formation of quartets and stacked quartets. The characteristic H(8) resonance feature at 8.05 ppm[4,6] indicating the presence of quartet assemblies is seen in Figure 5A. With temperature lowering, the main resonance indicated by χ in Figure 5A splits into four features labeled α, β, γ, and δ. With the decrease in temperature, the integrated areas of the α, β, and δ peaks increase, while that of the γ line decreases, reflecting the fraction of GMP incorporated into hydrogen-bonded assemblies. To within experimental uncertainty (±3%), integration of the α, β, and δ lines shows them to be of equal population. These data, therefore, show that the α, β, and δ peaks are caused by one type of stacked quartet, probably octets, as has been suggested by others.[44,45] Also at lower temperature, for example, at 1 °C, a small peak appears (ϵ) with a relative population of 4%, indicating a third type of aggregate. On the basis of NMR studies by others,[7,44] the sequential appearance of the χ; α, β, δ; and ϵ resonance peaks is indicative of monomers with quartets, octets, and dodecamers or other higher order aggregates, respectively. Hitherto, peak γ has not been assigned.

G-quartet formation was recently demonstrated by vibrational (Raman) spectroscopic methods for 1.0 M GMP solutions at pH 9.0,[9] and dynamic light scattering data show that the average size of stacked quartets can be over 2 units under these conditions.[10] From these studies we conclude that the α, β,

(42) Wasson, J. R. *Inorg. Chem.* **1971**, *10*, 1531–1534.

(43) A similar, direct comparison of the influence of metal ion concentration on the line width of the $-^5/_2$ parallel absorption feature cannot be carried out at pH 8.6 maintaining a constant GMP:VO^{2+} ratio of ~10:1 because changes in VO^{2+} or GMP concentration alter the relative quantities of G-quartets and stacked quartets from those formed at 0.01 M VO^{2+}.

(44) Borzo, M.; Detellier, C.; Laszlo, P.; Paris, A. *J. Am. Chem. Soc.* **1980**, *102*, 1124–1134.

(45) Bouhoutsos-Brown, E.; Marshall, C. L.; Pinnavaia, T. J. *J. Am. Chem. Soc.* 1982, *104*, 6576–6584.

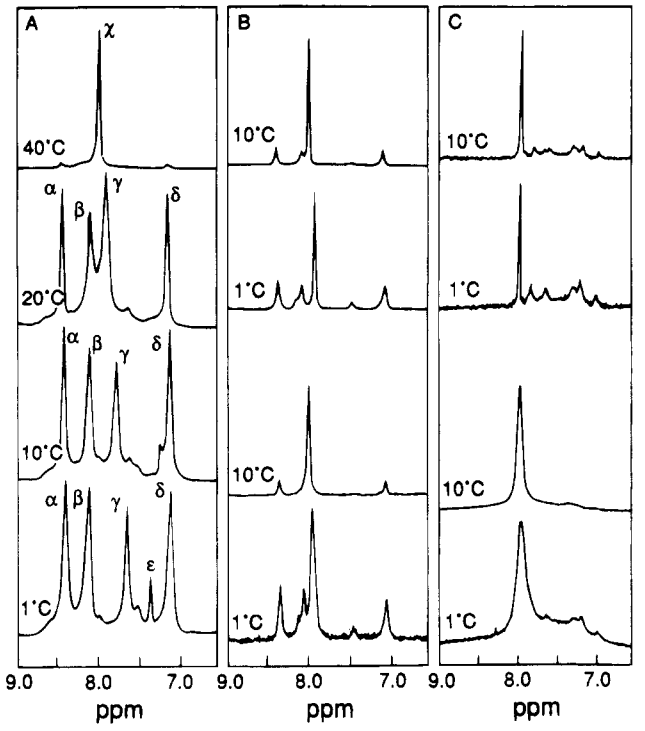

Figure 5. Comparison of ^{1}H NMR spectra in the H(8) region of GMP as a function of temperature and coordination to VO^{2+}. The chemical shifts are relative to [$^2H_6$]acetone as the internal standard: (A) 1.0 M GMP at pD 7.8; (B) 0.2 M GMP in 1.0 M NaCl at pD 8.8 (top two spectra) and 0.01 M VO^{2+} and 0.2 M GMP in 1.0 M NaCl at pD 8.8 (bottom two spectra); (C) 0.10 M GMP in 0.6 M KCl at pD 8.8 (top two spectra) and 0.04 M VO^{2+} and 0.10 M GMP in 0.6 M KCl solution at pD 8.8 (bottom two spectra). The temperature in °C is indicated for each spectrum.

and δ peaks represent the main components of the stacked quartets and that their integrated peak intensities represent an estimate of the extent of quartets becoming stacked quartets. On this basis, the results in Figure 5A show that for 1.0 M GMP at least 85% of the GMP has been incorporated into stacked quartet assemblies.

Corresponding ^{1}H NMR spectra of GMP in the presence of VO^{2+} are shown in Figure 5B,C under comparable solution conditions. Resonance features of [$VO(GMP)_2(H_2O)$] in 1.0 M NaCl at pD 8.8, seen in Figure 5B, are also observed, similar to those of VO^{2+}-free systems, indicating formation of quartets but with reduced formation of octets and higher order aggregates. Most importantly, by NMR, formation of quartets with reduced formation of stacked quartets was also observed in 0.6 M KCl at a GMP:VO^{2+} ratio of 2.5:1 (see Figure 5C). Under conditions of 2.5 M NaCl at pD 8.8, on the other hand, no evidence for stacked quartets was observed by NMR for solutions containing comparable mixtures of GMP and VO^{2+}. These observations agree with the results of Detellier and Laszlo[7] that potassium ions facilitate formation of stacked quartets. These observations, together with the results of EPR experiments described above, indicate that GMP complexed with VO^{2+} enters into self-structured quartet assemblies but that the tendency for formation of stacked quartets is reduced compared to that of GMP alone.

ENDOR Characterization of [$VO(GMP)_2(H_2O)$]. ENDOR, like NMR, is used to measure nuclear resonance absorption. ENDOR spectroscopy is performed at fixed magnetic field strength $\mathbf{H}_0$ by observing the change in the EPR signal intensity caused by nuclear resonance transitions induced through simultaneous irradiation of the sample with an rf field while an electronic transition is saturated under high levels of microwave power. The case of a paramagnetic metal ion with low g anisotropy presents a direct approach for structural analysis.[46,47] For a paramagnetic system of low g anisotropy, the first-order ENDOR transition frequencies $\nu_\pm$ within the strong-field approximation are given by eq 1, where $\nu_\pm$ represents the

$$\nu_\pm = \nu_n \pm |A|/2 \quad (1)$$

spacing of the pair of ENDOR features that appear symmetrically about the free nuclear frequency ν_n and A represents an orientation-dependent hf coupling.

The hf coupling may be described by eq 2 within the strong-field limit, where r is the electron−nucleus separation and α is

$$A = g_e \beta_e g_n \beta_n (3\cos^2 \alpha - 1)/hr^3 + A_{iso} \quad (2)$$

the angle between the electron−nucleus position vector $\mathbf{r}$ and the magnetic field $\mathbf{H}_0$. The first term in eq 2 corresponds to the dipole−dipole interaction yielding the dipolar hfc component A^D, and the second term A_{iso} is due to the Fermi contact interaction. The observed parallel and perpendicular hf splittings correspond to values of $\alpha = 0$ and 90°, respectively, and represent the principal hfc components $A_\parallel$ and $A_\perp$ of an axially symmetric hf matrix. Conditions ensuring that application of eq 2 for VO^{2+} systems is valid for $r \geq 2.5$ Å under the point-dipole approximation have been discussed previously.[48]

In previous studies using the vanadyl ion as a paramagnetic probe, we have described the principles of EPR angle selection for specifying molecular orientation in ENDOR spectroscopy and have discussed how ENDOR data are analyzed to specify molecular structure and conformation.[23,27,48] With respect to the vanadyl nucleotide complexes studied here, we select the $-^7/_2$ parallel EPR absorption feature for microwave saturation so that the molecular z axis coincident with the V=O bond is oriented parallel to $\mathbf{H}_0$, and correspondingly, we select the $-^3/_2$ perpendicular EPR absorption feature so that the field is perpendicular to the z axis or parallel to the molecular x,y plane. If a proton is located in an axial position with respect to the z axis of the VO^{2+} ion, then only $A_\parallel$ will be observed with the magnetic field set in the axial direction, and only $A_\perp$ will be observed with the magnetic field set in the g_x,g_y plane. If a proton is located in the g_x,g_y plane, then $A_\perp$ will be observed with the magnetic field set in the axial direction and both $A_\parallel$ and $A_\perp$ will be observed with the magnetic field set in the g_x,g_y plane. After $A_\parallel$ and $A_\perp$ have been determined, the dipolar hfc components $A_\parallel^D$ and $A_\perp^D$ are calculated under the constraints $A_\parallel > 0 > A_\perp$ and $(A_\parallel + 2A_\perp) = 3A_{iso}$.

Figures 6 and 7 illustrate proton ENDOR spectra for $\mathbf{H}_0$ settings at the $-^3/_2$ perpendicular and $-^7/_2$ parallel EPR absorption features, respectively. Under the solution conditions described, the fraction of stacked quartets was less than 5% as assessed on the basis of NMR spectra. In Table 1 we have summarized the values of the ENDOR line splittings and their assignments. Proton resonance absorption features were first assigned according to their sensitivity to solvent exchange and spectroscopic character. Thus, the resonance features S1 and S2 are assigned to the VO^{2+}-bound water in an axially coordinated position *trans* to the V=O group,[23] and resonances B1 and B2 are assigned to a solvent-exchangeable, axially located proton on the GMP moiety. On the other hand, the

(46) Hurst, G. C.; Henderson, T. A.; Kreilick, R. W. *J. Am. Chem. Soc.* **1985**, *107*, 7294−7299.
(47) Henderson, T. A.; Hurt, G. C.; Kreilick, R. W. *J. Am. Chem. Soc.* **1985**, *107*, 7299−7303.
(48) Makinen, M. W.; Mustafi, D. In *Metal Ions in Biology*; Sigel, H., Ed.; Marcel Dekker: New York, 1994; Vol. 31, pp 89−127.

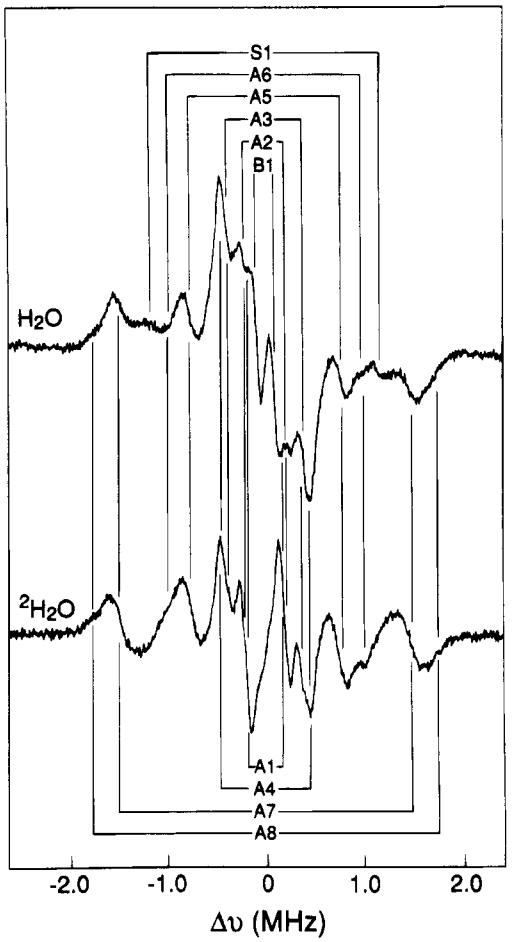

Figure 6. Proton ENDOR spectra of $[VO(GMP)_2(H_2O)]$ with $\mathbf{H}_0$ at the $-3/2$ perpendicular EPR setting. The line pairs denoted by symbols A and B belong to nonexchangeable and exchangeable protons of the bound GMP moiety, respectively, while S denotes resonances of solvent protons. Solution conditions were 0.01 M VO^{2+} and 0.1 M GMP in 1.0 M NaCl solution at pH 8.6 in H_2O (top spectrum) and at pD 8.6 in ^2H_2O (bottom spectrum).

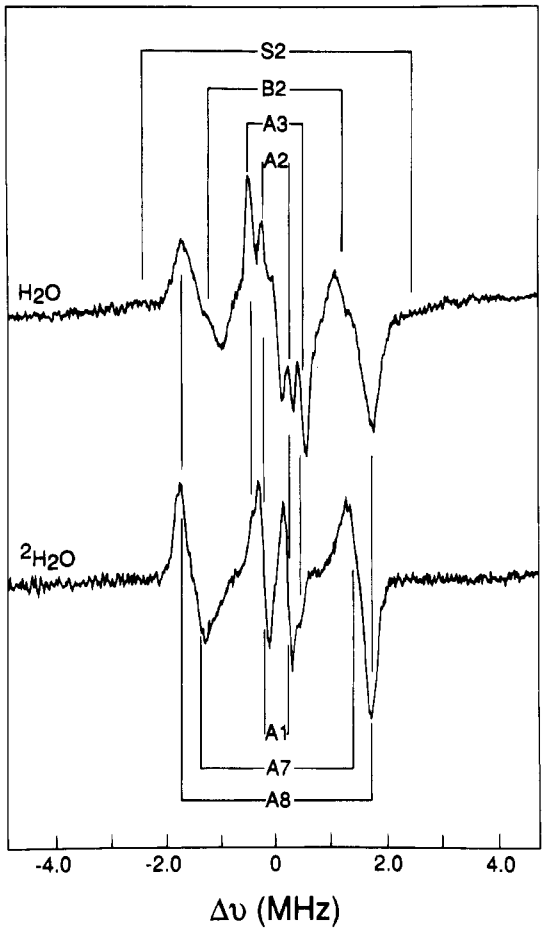

Figure 7. Proton ENDOR spectra of the $[VO(GMP)_2(H_2O)]$ complex with $\mathbf{H}_0$ at the $-7/2$ parallel EPR setting. Other conditions were as in Figure 6.

line pairs A1 and A4 derive from H(8) because these features were absent for GMP heated in ^2H_2O, as described under Experimental Procedures. Since resonance features A1−A3 are observed for both $-7/2$ parallel and $-3/2$ perpendicular settings and A4−A6 occur only with $\mathbf{H}_0$ at the $-3/2$ perpendicular setting, we assign the A1−A3 line pairs to perpendicular hfc components and A4−A6 to parallel hfc components of nucleotide protons located in or very close to the equatorial plane of donor ligands. The pairing of parallel and perpendicular resonance features was assigned so as to yield the smallest absolute value of A_{iso}. The line pairs A7 and A8 are unusual in that they were observed with $\mathbf{H}_0$ set at the $-3/2$ perpendicular and $-7/2$ parallel features, but the signal of A7 was much stronger with $\mathbf{H}_0$ set to the $-3/2$ perpendicular EPR feature. The signal intensity of A8 showed a reversed relationship. We conclude that these latter two sets of ENDOR features derive from a proton that is positioned intermediate between a purely axial and a purely equatorial position but near the molecular z axis.

On the basis of NMR spectra of solutions containing 0.2 M GMP with only 0.01 M VO^{2+} in 1.0 M NaCl buffered to pD 8.8, the fraction of GMP in stacked quartets was estimated as at least 65%. Under these conditions, the proton ENDOR spectra were indistinguishable from those in which less than 5% of the nucleotide had formed stacked quartets. Under conditions of a GMP:VO^{2+} ratio of 2.5:1 with about 50% of GMP in stacked quartets, the same proton ENDOR absorption features with identical splittings were also observed although the ENDOR signals were much weaker than when formed at high NaCl concentration and a GMP:VO^{2+} ratio of 10:1. The weaker signals may have their origin either in the increased spin−spin interactions of the VO^{2+} ions through nearest neighbor effects or in the glass-forming properties of KCl solutions compared to those of NaCl solutions.

Table 1. Observed Proton ENDOR Splittings of the $[VO^{2+}(GMP)_2(H_2O)]$ Complex in Frozen Solutions of 0.01 M VO^{2+}, 0.1 M GMP, and 1.0 M NaCl at pH (or pD) 8.6

$\mathbf{H}_0$ setting	line pairs[a]	line splittings[b]	assignments[c]
$-3/2\perp$ $-7/2\parallel$	A1	0.33	GMP equa
$-3/2\perp$ $-7/2\parallel$	A2	0.35	GMP equa
$-3/2\perp$ $-7/2\parallel$	A3	0.78	GMP equa
$-3/2\perp$	A4	0.94	GMP equa
$-3/2\perp$	A5	1.58	GMP equa
$-3/2\perp$	A6	2.01	GMP equa
$-3/2\perp$ $(-7/2\parallel)$	A7	2.82	GMP near axial
$-7/2\parallel$ $(-3/2\perp)$	A8	3.51	GMP near axial
$-3/2\perp$	B1	0.17	GMP exch axial
$-7/2\parallel$	B2	2.12	GMP exch axial
$-3/2\perp$	S1	2.30	solvent (axial H_2O)
$-3/2\parallel$	S2	5.08	solvent (axial H_2O)

[a] Line pairs are assigned in Figures 6 and 7. [b] Since hf couplings were measured as the frequency difference between the two components of a line pair and the signal-to-noise ratio was comparable for most ENDOR lines, the estimated uncertainty in the splitting is considered as $\sigma/2$, where σ is the standard deviation or one-half of the full line width (ΔH_{pp}) between the extrema of the first-derivative curve.[41] On this basis, the estimated uncertainties are 3−4%. [c] equa = equatorial; exch = exchangeable.

In addition to ^1H ENDOR, we have also observed ^{31}P ENDOR, as in earlier studies.[27] With $\mathbf{H}_0$ at the central, prominent absorption feature, two distinct ENDOR resonance features were observed at 22.9 and 34.4 MHz in both H_2O and ^2H_2O solutions containing 0.01 M VO^{2+} and 0.1 M GMP, in buffered 1.0 M NaCl. In this case, the central, prominent EPR feature was used for the $\mathbf{H}_0$ setting because it shows the largest peak-to-peak amplitude (*cf.* Figure 2). The two ^{31}P resonance features were thus separated by 11.5 MHz. According to the relationship $\nu_\pm = |A|/2 \pm 2\nu_n$, applicable for the condition of $\nu_n \leq |A|/2$ as in the case of the ^{31}P nucleus, the ^{31}P ENDOR spectra yield an estimate of 57.4 MHz for the hfc constant of the ^{31}P nucleus. This is in good agreement with the value of 58.9 MHz estimated on the basis of the EPR superhyperfine coupling features in Figure 4.

Molecular Modeling of $[VO(GMP)_2(H_2O)]$. For assignment of the structure and conformation of the $[VO(GMP)_2(H_2O)]$ complex, a molecular model was derived first on the basis of X-ray-defined molecular fragments. The structure of the complex is based on the spectroscopic observations of (i) a GMP:VO^{2+} stoichiometry of 2:1; (ii) evidence for only an axially coordinated water molecule; and (iii) the superhyperfine coupling pattern attributable to ^{31}P, requiring two phosphate groups coordinated in structurally equivalent positions. The latter observation, therefore, positions both phosphate groups as coordinated in the equatorial plane through oxygen atoms. Since no solvent molecules in equatorial coordination sites could be detected, each phosphate group must coordinate the VO^{2+} ion in a bidentate configuration. A similar coordination geometry has been assigned to bis(*O,O'*-dialkyl dithiophosphato)oxovanadium(IV) complexes on the basis of analysis of infrared absorption and EPR-determined hfc patterns.[42,49] It is also of interest to note that VO^{2+} can be specifically substituted into Ca^{2+} binding sites.[38,50] Bidentate chelation of Ca^{2+} ions by phosphate groups has been described through X-ray studies.[51]

To model the bidentate coordination of each phosphate group, we employed the X-ray-defined structure of $NaV_3P_3O_{12}$,[30] in which vanadium atoms are coordinated equatorially so as to form two V−O−P−O tetragonal units in a 2-fold symmetric manner. For the bidentate coordination of the V=O group by the 5′-phosphate group of GMP, the two equatorial V−O bonds were made equivalent at 2.048 Å in length and the two P−O bonds were 1.58 Å in length, the O−V−O and O−P−O vertices defining valence angles of 76.5 and 110.0°, respectively. On the other hand, the other two P−O bonds of each phosphate group were assigned bond lengths of 1.50 and 1.58 Å, respectively, the latter corresponding to the bridging oxygen attached to the 5′-methylene group of the ribose moiety. In the structure of $NaV_3P_3O_{12}$, the O−V−O and O−P−O valence angles are 69.9 and 97.6°, respectively.[30] We were unable to accommodate a single phosphate group in this exact geometry without distortion of the valence angles observed in GMP·$3H_2O$. Since the structure of $NaV_3P_3O_{12}$ is of a polyphosphate complex containing VO_6 octahedra, it may be expected to exhibit altered structural parameters with respect to O−P−O and O−V−O valence angles. We, therefore, superposed the phosphate groups of GMP onto the $NaV_3P_3O_{12}$ structure with as little stereochemical distortion as possible to the 5′-phosphate group. We have no evidence of unusual geometrical strain in the bis(phosphate)-coordinated vanadyl unit.[52]

After assigning the coordination structure of VO^{2+} in the $[VO(GMP)_2(H_2O)]$ complex, we then searched for plausible conformations of the guanosyl−ribose moiety that could account for the five protons observed by ENDOR. This analysis was performed on the basis of the torsion angle search calculations with rotation around the C(1′)−N(9), C(5′)−C(4′), C(5′)−O(5′), O(5′)−P, C(2′)−O(2′), and C(3′)−O(3′) bonds. The chemical bonding structure and atomic numbering scheme for GMP together with the four torsion angles are illustrated in Figure 1. The search calculation was started with the *C3′-endo* ribose pucker and two proton distance constraints: a 5.65 Å metal−proton distance to H(8) and a 4.64 Å distance to H(O2′). The results gave a family of conformers in which the metal−proton distances for H(1′), H1(5′), and H(4′) were consistent with the ENDOR-determined distances of 4.92, 4.35, and 3.31 Å, respectively, in addition to the assigned distances of 5.65 Å to H(8) and 4.64 Å to H(O2′). Furthermore, the orientations of these protons also agree with those determined by ENDOR with respect to angle-dependent hfc patterns. The values of the ENDOR-constrained torsion angles are compared in Table 3. The family of conformers that were accommodated by the ENDOR-determined distances with their respective uncertainties were consistent with only an *anti* conformation about the C(1′)−N(9) bond with a torsion angle χ of 185 ± 10°. The ENDOR-based molecular structure of $[VO(GMP)_2(H_2O)]$, reflecting the metal−proton distances and torsion angles listed in Tables 2 and 3, is illustrated in Figure 8.

When the exchangeable proton with a 4.64 Å metal−proton distance was assigned to H(O3′) with a *C3′-endo* ribose pucker,

Table 2. Principal Proton Hyperfine Coupling Constants (A, MHz) and Calculated Metal−Proton Distances (r, Å) in the $[VO(GMP)_2(H_2O)]$ Complex

$A_\parallel^{obs}$	$A_\perp^{obs}$	A_{iso}	$A_\parallel^{D}$	$A_\perp^{D}$	r^a	proton assignment[b]
0.94	0.33	0.09	0.85	−0.42	5.65	Gua H(8)
1.58	0.35	0.29	1.29	−0.65	4.92	Rib H(1′)
2.01	0.78	0.15	1.86	−0.93	4.35	Rib H1(5′)
2.12	0.17	0.59	1.53	−0.76	4.64	Rib H(O2′)
3.51	2.82	−0.71	4.22	−2.11	3.31	Rib H(4′)
5.08	2.30	0.16	4.92	−2.45	3.15[c]	axial H_2O

[a] The uncertainties in r are 0.10−15 Å based on the estimated uncertainty in measurement of hf couplings. [b] The completed assignments of these protons are based on ENDOR determinations and molecular modeling studies as discussed in the text. [c] The vanadium−proton distance for the axially located water molecule is longer than that (2.9 Å) observed in $[VO(H_2O)_5]^{2+}$ or in $[VO(ADP)_2(H_2O)]$ at lower pH.[23,27] Also, the resonance features S1 and S2 (*cf.* Table 1) are less prominent than those for axially coordinated water at lower pH. However, essentially identical resonance features were observed for VO^{2+} at pH ≥12 (Jiang, F. S., Makinen, M. W. Unpublished observations) to which the spectrum of $[VO(GMP)_2(H_2O)]$ is similar, as described in the text. Ianuzzi and Rieger have pointed out that at pH >12 the EPR spectrum of VO^{2+} shows increased covalency of equatorial ligands.[40] This effect would be expected to "tighten" the equatorial metal−ligand bonds and increase slightly the bond length to the axially positioned water molecule.

Table 3. Torsional Angles (deg) of $[VO(GMP)_2(H_2O)]$ Determined by ENDOR-Constrained Molecular Modeling

torsional angle	τ
α [O(6′)−P−O(5′)−C(5′)]	27 ± 5
β [P−O(5′)−C(5′)−C(4′)]	272 ± 4
γ [O(5′)−C(5′)−C(4′)−C(3′)]	227 ± 5
χ [O(4′)−C(1′)−N(9)−C(4)]	185 ± 10
[H(2′)−C(2′)−O(2′)−H(O2′)]	185 ± 30

(49) Miller, G. A.; McClurg, R. E. D. *Inorg. Chem.* **1973**, *12*, 2552−2561.
(50) Mustafi, D.; Nakagawa, Y. *Proc. Natl. Acad. Sci. U.S.A.* **1994**, *91*, 11323−11327.
(51) MacLennan, G.; Burns, C. A. *Acta Crystallogr.* **1956**, *9*, 187−190.

(52) Wasson[42] discusses variation of the valence angle involving the central ^{31}P atom of a bidentate coordinating phosphate group as a function of the strength of the isotropic hfc interaction with the V^{4-} cation. The isotropic hfc for $[VO(GMP)_2(H_2O)]$ due to ^{31}P falls into the low end of the range observed for bis(dithiophosphato)oxovanadium(IV) chelates.

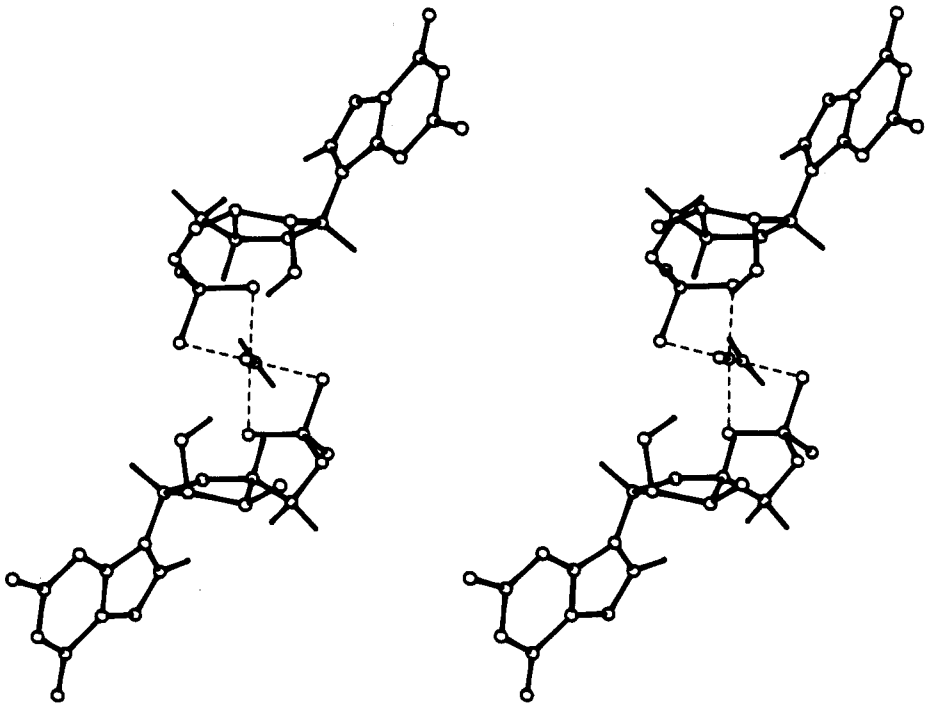

Figure 8. Stereodiagram of the structure of $[VO(GMP)_2(H_2O)]$ determined on the basis of EPR and ENDOR spectroscopy and molecular modeling. Dotted lines connect V(IV) to the phosphate oxygens of the two symmetry-related, equatorially positioned GMP moieties and to the axially positioned water molecule. The ENDOR-determined hydrogen atom positions of H(8), H(1′), H(O2′), H(4′), H1(5′), and the axially coordinated H_2O are shown, in addition to non-hydrogen atoms.

no conformer was found to accommodate the ENDOR-determined metal−proton distances. Also, there was no *C3′-endo* conformation which allowed the assignment of the exchangeable proton with a 4.64 Å metal−proton distance to N(1) or N(2). Since the *C2′-endo* conformation of the ribose unit is the other predominant structure of monoribonucleotides in solution, the *C2′-endo* ribose puckering mode was also considered in the search calculations. With metal−proton distances of 5.65 Å assigned to H(8) and 4.64 Å to H(O2′), a limited, small set of conformers was identified which accommodated the other metal−proton distance constraints but whose positions did not correspond to the requirements of the angle-selected ENDOR-determined hfc patterns. Furthermore, this structure would have placed one of the two GMP units of the complex so as to sterically prevent formation of stacked quartets, as discussed later. This structure was, therefore, ruled out. There were no *C2′-endo* conformers which allowed the assignment of a 4.64 Å metal−proton distance to the exchangeable H(O3′) or H(N1) or to H(N2)1 or H(N2)2. The final results, thus, show that the ENDOR data for $[VO(GMP)_2(H_2O)]$ complex are compatible only with an *anti* base conformation and a *C3′-endo* ribose pucker. This is consistent with X-ray data which show that the *C3′-endo* pucker usually corresponds to the *anti* conformation.[53,54]

Conformational Analysis of Self-Structured Assemblies of GMP with $[VO(GMP)_2(H_2O)]$. Figure 9 illustrates the molecular model of structural relationships of a $[VO(GMP)_2(H_2O)]$ complex incorporation into a G-quartet. The basic structural relationships of the quartet of hydrogen-bonded guanine bases are derived from the X-ray structure of $d(G_4T_4G_4)$.[14] The structure of $[VO(GMP)_2(H_2O)]$ is directly taken as the ENDOR-constrained model described above. Since the ENDOR spectra are identical for all aggregation states of $[VO(GMP)_2(H_2O)]$, including conditions favoring only monomers or primarily quartets and stacked quartets, we conclude that, even under conditions of incorporating more than one $[VO(GMP)_2(H_2O)]$ unit into a quartet, the base and ribose conformations remain unchanged. Estimates of the EPR line width showed evidence of spin−spin interactions for low ratios of GMP to VO^{2+}, i.e., less than 4:1. On this basis, we have evaluated the inter-vanadyl distances for G-quartets containing more than one $[VO(GMP)_2(H_2O)]$ unit. Within the structure as illustrated in Figure 9, the inter-vanadyl separations would correspond to 16−18 Å along an edge with diagonal distances between two VO^{2+} ions of 24−25 Å.[55] Such inter-vanadyl distances could give rise to spin−spin interactions resulting in an increase in EPR line width.[56]

Although biological examples of G-quartets in RNA are not known at present, it is likely that they will be found, given the tendency of guanine to hydrogen-bond with itself to form stable arrays. Our ENDOR results may provide insight into the probable conformation of guanosine units in quartets formed within RNA molecules. The precision of our ENDOR-based estimates of metal−proton distances in Table 2 accommodate only a *C3′-endo* ribose structure with an *anti* conformation of the glycosidic bond. We conclude that, for GMP in solution, this ribose conformation obtains for all GMP units coordinated

(53) de Leeuw, H. P. M.; Haasnoot, C. A. G.; Altoma, C. *Isr. J. Chem.* **1980**, *20*, 108−126.

(54) Saenger, W. *Principles of Nucleic Acid Structure*; Springer-Verlag: New York, 1984; Chapter 4, pp 51−104.

(55) Inter-vanadyl distances between stacked quartets would be expected to be comparable since it is unlikely sterically for two $[VO(GMP)_2(H_2O)]$ units from adjacent stacked quartets to be aligned side-by-side. A distance shorter than 16−18 Å along the edge of stacked quartets could occur also, depending on "stagger" of two adjacent quartet units.

(56) The deviations in the electron energy levels of a paramagnetic site with $S = {}^1/_2$ due to the dipolar field of another unpaired electron at a distance of ~20 Å will result in a line width of ~4 G.[41] Thus, a separation ≤16−18 Å is consistent with the observed approximate 6 G increase in the EPR line width of the $-{}^5/_2$ parallel absorption feature described above for mixtures of GMP:VO^{2+} ratios of ~2.5:1. Since the dipolar broadening between vanadyl units is likely to occur simultaneously within a quartet as well as between quartets for GMP:VO^{2+} ratios of ~2.5:1, the extent of line width broadening with inter-vanadyl distance cannot be quantified more precisely.

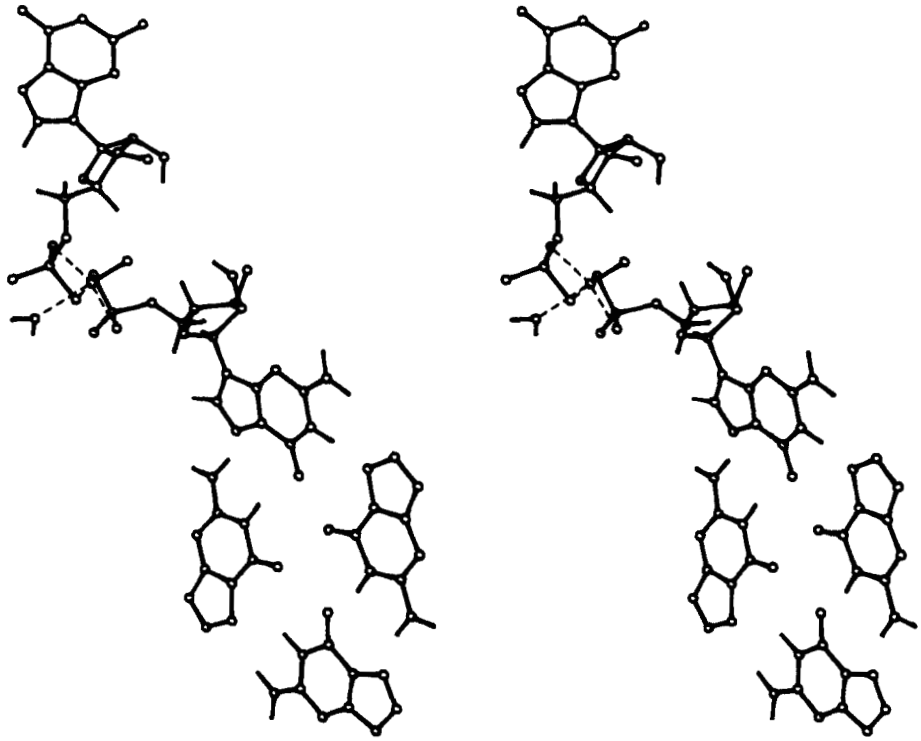

Figure 9. Stereodiagram of $[VO(GMP)_2(H_2O)]$ incorporated into a G-quartet on the basis of molecular modeling. The constraints placing the vanadyl–nucleotide complex into a G-quartet are discussed in the text.

to the VO^{2+} and incorporated into G-quartets and higher order assemblies. High-resolution NMR studies have shown that an *anti* conformation of the guanine bases is associated with a *C3'-endo* ribose pucker in more than 75% of the guanosine units in G-quartets formed within the tetraplex structure of $(rUGGGGU)_4$.[15] These results, thus, suggest that G-quartets in RNA are likely to be primarily associated with an *anti* conformation of the glycosidic bond and a *C3'-endo* conformation of the ribose unit. On the other hand, X-ray[14] and NMR[16] studies show that G-quartet formation in strands of the oligonucleotide $d(G_4T_4G_4)$ is associated with alternate *syn* and *anti* conformations of the guanine base along each strand with all ribose units exhibiting the *C2'-endo* ribose pucker. In contrast, the guanine bases in the quadruplex structures of the human telomere sequence $d(T_2AG_3)$ and the tetrahymena telomere sequence $d(T_2G_4)$ are all found in an *anti* conformation.[17] In the latter two types of G-quartets formed from deoxynucleotide strands, a *C3'-endo* conformation of the ribose groups is not observed.

Acknowledgment. We thank Dr. D. Mustafi for helpful discussions and Professor A. Rich for communication of the atomic coordinates of $d(G_4T_4G_4)$.

IC9409266